Preisach Modelling: Symmetry Implementation and Frequency Analysis

Mårten Sjöström

Swiss Federal Institute of Technology, Lausanne, Switzerland

Abstract

The paper contains an analysis of the classical Preisach model from a symmetry and a frequency point of view. Increasing and decreasing inputs have no fundamental difference, which leads to a simplified implementation by changing indices. Symmetry implies that the fully demagnetised state can be taken into account without approximations. A frequency analysis demonstrates that all odd and only odd harmonics of the fundamental input frequency are transferred to the output. As a consequence an estimation method for the Preisach model weighting function from sinusoidal input is suggested

Keywords

Preisach model, hysteresis, implementation, Fourier analysis, parameter estimation

I. Introduction

HYSTERESIS can generally be described as a hysteresis transducer with an input signal $u(t)$ and an output signal $y(t)$ and is widely modelled with a Preisach model [1]–[2]. It is now used in a wide range of scientific areas to describe hysteresis, and so it is exhaustively discussed in large number of papers and books, for instance [3]–[7].

In this paper, the classical Preisach model is considered. By remarking that there is no fundamental difference of increasing and decreasing input, a simple change of indices highly simplifies the coding of an implementation. Both the output signal $y(t)$ and the instantaneous energetic losses $Q(t)$ are computed in this fashion. Furthermore, the suggested implementation allows any 'magnetisation' as starting value and takes the the fully 'demagnetisation state' into account with no approximation when symmetry applies.

A frequency analysis is carried out with an arbitrary weighting function. It shows that the output contains all odd harmonics of the fundamental input frequency. A numerical simulation further demonstrates that the output contains only odd harmonics. These results justify an extraction of all odd harmonics above noise level as filtering of time-series measurements with sinusoidal input. As a consequence, a novel identification method is suggested for the Preisach model weighting function which uses sinusoids of different amplitudes as input, however different from the identification method in [4]. It is simpler than the conventional first-transition curve identification (described in [3]).

A good description of the classical Preisach model of hysteresis is found in [3]. The notation is here slightly changed and the simplest hysteresis operator has been given a unit step centred around zero. Therefore, the paper starts by describing the Preisach model, which also facilitates the comprehension of the following parts that contain the description of the numerical implementation and the frequency analysis.

II. The Preisach Model

The Preisach model consists of a superposition of an infinite number of simplest hysteresis operator $\zeta_{\mathrm{L}\Gamma}$, each representing a rectangular loop in the output-input $(y-u)$ diagram, see Fig. 1. The output of the simplest hysteresis operator can take values $\pm 1/2$ only, where Γ and L correspond to the 'up'

M. Sjöström, CIRC-EPFL, CH-1015 Lausanne, Switzerland, tel (+41-21) 693-5684, fax (+41-21) 693-6700, email Marten.Sjostrom@epfl.ch, http://circwww.epfl.ch

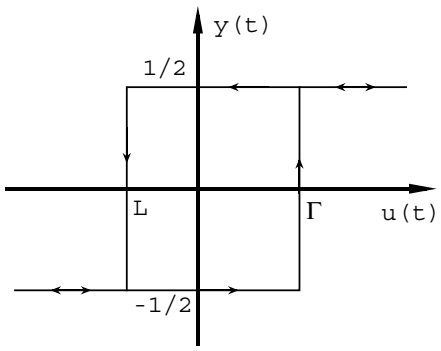

Fig. 1. The output due to the simplest hysteresis operator $\zeta_{\mathrm{L}\Gamma}$ is a rectangular loop in the output-input diagram which possesses an 'up'-switch at Γ and a 'down'-switch at L.

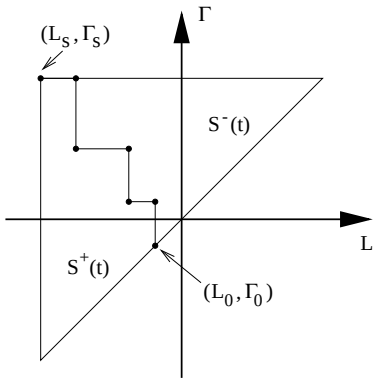

Fig. 2. Geometric interpretation of the Preisach model. The half-plane $\Gamma \geq \mathrm{L}$ is divided by $\mathcal{C}(t)$ into two parts where $\zeta_{\mathrm{L}\Gamma}$ is positive and negative respectively.

and 'down' switching, respectively. In the sequel, it is assumed that $\Gamma \geq \mathrm{L}$. Each $\zeta_{\mathrm{L}\Gamma}$ is weighted by an arbitrary weighting function $w(\mathrm{L}, \Gamma)$, leading to the following expression for the Preisach model:

$$y(t) = \iint w(\mathrm{L}, \Gamma)\zeta_{\mathrm{L}\Gamma}[u(t)]d\Gamma d\mathrm{L} \tag{1}$$

The Preisach model can be interpreted geometrically, since there is a one-to-one correspondence between the $\zeta_{\mathrm{L}\Gamma}$ and the point (L, Γ). The half-plane $\Gamma \geq \mathrm{L}$ is only considered. When the output of the hysteresis transducer has a saturation, the $\mathrm{L} - \Gamma$ plane has a horizontal and a vertical limiting line, outside of which the weighting function is equal to zero. This limiting triangle T is bordered by the line $\mathrm{L} = \Gamma$ and has a right angle at the vertex (L_s, Γ_s), see Fig. 2.

There is a subdivision of T into $S^+(t)$ and $S^-(t)$, the two parts where $\zeta_{\mathrm{L}\Gamma}$ is positive and negative respectively. This division depends on extrema of past input and on the present input, and consists of a line $\mathcal{C}(t)$. Its last value (L_0, Γ_0) corresponds to the present value of the input $(u(t), u(t))$ and is attached to the line $\mathrm{L} = \Gamma$ in the figure. The subdivision of T is along the line $\mathrm{L} = -\Gamma$ when the hysteresis transducer has no memory, but when the input has reached certain levels, $\mathcal{C}(t)$ makes a 'stair-case' line. This means that the memory consists of a number of vertices, e.g.

$$\mathcal{C}(t) = \{(\mathrm{L}_s, \Gamma_s), \cdots, (\mathrm{L}_1, \Gamma_2), (\mathrm{L}_1, \Gamma_1), (\mathrm{L}_0, \Gamma_1), (\mathrm{L}_0, \Gamma_0)\}. \tag{2}$$

It is clear that $\mathcal{C}(t)$ constantly changes with time (i.e. if $u(t)$ changes with time) and hence $S^+(t)$ and $S^-(t)$ also change. The output of the hysteresis transducer then takes the following form:

$$y(t) = \frac{1}{2}\iint\limits_{S^+(t)} w(\mathrm{L}, \Gamma)d\Gamma d\mathrm{L} - \frac{1}{2}\iint\limits_{S^-(t)} w(\mathrm{L}, \Gamma)d\Gamma d\mathrm{L}\,. \tag{3}$$

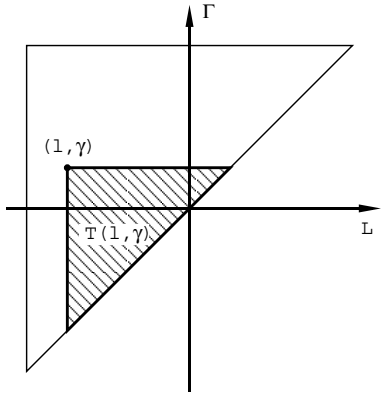

Fig. 3. The triangle that is limited by L=Γ and the coordinate (l, γ) as in the figure defines the surface over which the weighting function is integrated to form the function $W(l, \gamma)$.

since $\zeta_{\mathrm{L}\Gamma}[u(t)]$ takes the values $+1/2$ and $-1/2$ in $S^+(t)$ and $S^-(t)$ respectively.

If the input increases beyond a memory vertex in the graph, i.e. $u(t) < \mathrm{L}_i$ or $u(t) > \Gamma_i$, that particular vertex is wiped out from the history $\mathcal{C}(t)$. The model (3) also implies that a periodic input results in congruent minor hysteresis loops independent of the history $\mathcal{C}(t)$. The erasing of extrema and the congruency of minor loops are the necessary and sufficient properties of a physical hysteresis to be described by the Preisach model [3].

Instead of the weighting function $w(\mathrm{L}, \Gamma)$, we can use the function $W(l, \gamma)$ which is the integral of $w(\mathrm{L}, \Gamma)$ over a triangular domain $T(l, \gamma)$ as the one presented in Fig. 3,

$$W(l, \gamma) \stackrel{\text{def}}{=} \iint\limits_{T(l,\gamma)} w(\mathrm{L}, \Gamma) d\Gamma d\mathrm{L}\,, \tag{4}$$

with the inverse formula

$$w(\mathrm{L}, \Gamma) = -\frac{\partial^2}{\partial\Gamma\partial\mathrm{L}}\, W(\mathrm{L}, \Gamma)\,. \tag{5}$$

By using (3), it is seen that $W(l, \gamma)$ is equal to the difference of the output:

$$W(l, \gamma) = W(u(t_l), u(t_\gamma)) = y(t_\gamma) - y(t_l)\,, \tag{6}$$

for a history $\mathcal{C}(t)$ such that $\Gamma_i > \gamma, \mathrm{L}_i > l\, \forall i$, and so $W(l, \gamma)$ can be retrieved directly from measured output. There are certain advantages for the use of $W(l, \gamma)$, such as the calculation of double integrals is replaced by the calculation of finite sums in an implementation, see Section III

On physical grounds (symmetry considerations), it can be expected that the decreasing and increasing transition curves are congruent, which then has the consequence that

$$W(l, \gamma) = W(-\gamma, -l) \quad \text{and} \quad w(\mathrm{L}, \Gamma) = w(-\Gamma, -\mathrm{L})\,. \tag{7}$$

The symmetry relation (7) is used in the numerical implementation in Section III and in the Fourier analysis in Section IV.

In particular applications the derivative of the output from the Preisach model is the sought measure, which we denote by

$$v(t) = \frac{dy(t)}{dt}\,. \tag{8}$$

A. Energy Losses

It is well known that hysteresis phenomena are associated with some energy dissipation where hysteretic energy losses are equal to the area enclosed by a loop resulting from a periodic input.

Returning to the simplest hysteresis operator $\zeta_{\mathrm{L}\Gamma}$ and its representation in the output-input diagram (Fig. 1), it is realised that the horizontal lines are reversible and hence give no energy loss. Therefore, the 'up' and 'down' switching contains all energy dissipation. Symmetry considerations leads to assigning equal loss per switching [3],

$$q = \frac{1}{2}(\Gamma - \mathrm{L})\,. \tag{9}$$

The energy losses for a monotonic increase of input $u_1 \to u_2$ can therefore be calculated by integrating q weighted by $w(\mathrm{L},\Gamma)$ over a surface S in the Γ-L diagram,

$$Q(u_1,u_2) = \frac{1}{2}\iint\limits_S w(\mathrm{L},\Gamma)(\Gamma-\mathrm{L})d\Gamma d\mathrm{L}\,. \tag{10}$$

The energy loss for any closed loop of a monotonically increasing and then monotonically decreasing input between the values u^- and u^+ has the following expression

$$Q_c(u^-,u^+) = \iint\limits_{T(u^-,u^+)} w(\mathrm{L},\Gamma)(\Gamma-\mathrm{L})d\Gamma d\mathrm{L}\,, \tag{11}$$

where $T(u^-,u^+)$ is the triangular surface in the L-Γ plane swept by the input signal during one cycle, c.f. Fig. 3. An inverse formula can be derived from (11) by which the weighting function $w(\mathrm{L},\Gamma)$ can be calculated from a known energy loss per cycle [5]:

$$w(\mathrm{L},\Gamma) = -\frac{1}{\Gamma-\mathrm{L}}\,\frac{\partial^2}{\partial\mathrm{L}\partial\Gamma}\,Q_c(\mathrm{L},\Gamma) \tag{12}$$

The formula (12) tells us that when the energy losses can be expressed analytically for a loop, the Preisach model can be derived with exact losses [6]. The derived weighting functions $w(\mathrm{L},\Gamma)$ and $W(l,\gamma)$ then enable simulations of such systems for an arbitrary input.

The use of $W(l,\gamma)$ implies, by partial integration, an expression for the energy loss (10) over the triangle $T(u^-,u^+)$ [3] as

$$Q_W(u^-,u^+) = \frac{1}{2}(u^+-u^-)W(u^-,u^+) - \frac{1}{2}\int_{u^-}^{u^+} W(l,u^+)dl - \frac{1}{2}\int_{u^-}^{u^+} W(u^-,\gamma)d\gamma\,. \tag{13}$$

The loss by such a monotonic increase of the input equals the loss for the corresponding decrease. In the case when the loop is between two input values that are symmetrically placed around zero, e.g. in the case of the sinusoidal input signal with peak value U_0,

$$u(t) = U_0\cos(\omega_0 t)\,, \tag{14}$$

and symmetry (7) applies, the hysteretic losses of a full loop are expressed by

$$Q_c(-U_0,U_0) = 2U_0W(-U_0,U_0) - 2\int_{-U_0}^{U_0} W(l,U_0)dl\,. \tag{15}$$

The above formula is useful when relating a parametrised $W(l,\gamma)$ and measured energy losses, so that the parameters can be identified as in [7]

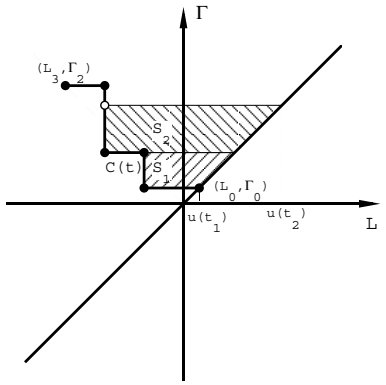

Fig. 4. The numerical implementation of the Preisach model involves integration of a number of surfaces, Q_k. In the case where there exists a hysteresis memory, these surfaces are differences of triangles, so that $W(l,\gamma)$ can be used.

III. Numerical Implementation

The Preisach model can be numerically implemented directly by applying the integral (3), or by using the function $W(l,\gamma)$ in (4), c.f. [3]. Here the fact that there is no fundamental difference between an increasing ($du/dt > 0$) or a decreasing input signal ($du/dt < 0$) is used; it just corresponds to a change of indices. This is used to simplify an implementation. This technique works for both the output signal $y(t)$ and the energetic losses $Q(t)$. A fully demagnetised state where the material has no memory is treated as such, with no approximations when symmetry (7) applies. The following simplification of notation is applied:

$$u(t_i) = u_i\,, \qquad y(t_i) = y_i\,. \tag{16}$$

A. The Output y(t)

First, assume a situation as in Fig. 4 or 5 where the memory function consists of the vertices

$$\mathcal{C}(t) = \{(\mathrm{L}_3,\Gamma_2),(\mathrm{L}_2,\Gamma_2),(\mathrm{L}_2,\Gamma_1),(\mathrm{L}_1,\Gamma_1),(\mathrm{L}_1,\Gamma_0),(\mathrm{L}_0,\Gamma_0)\}. \tag{17}$$

The difference of the output at arbitrary times $t_2 > t_1$ is then a sum of integrals over the surfaces S_1 and S_2, or generally:

$$\Delta y_2 = y_2 - y_1 = \sum_{k=1}^{n(t)} \iint\limits_{S_k(t)} w(\mathrm{L},\Gamma)\,d\Gamma\,d\mathrm{L}\,. \tag{18}$$

Henceforth, the dependence of time for $n(t)$ and $S_k(t)$ will not be expressed explicitly. The surface S_k is equal to the difference of two triangular surfaces so that the integrals in (18) can be calculated as differences of integrals over triangular surfaces. But the values of these integrals were defined to be the function $W(l,\gamma)$, and the expression (18) can be simplified to be a sum of differences:

$$\begin{aligned}\Delta y_2 = \sum_{k=1}^{n-1} &\Big(\iint\limits_{T(\mathrm{L}_k,\Gamma_k)} w(\mathrm{L},\Gamma)\,d\Gamma\,d\mathrm{L} - \iint\limits_{T(\mathrm{L}_k,\Gamma_{k-1})} w(\mathrm{L},\Gamma)\,d\Gamma\,d\mathrm{L}\Big) \\ &+ \Big(\iint\limits_{T(\mathrm{L}_n,u_2)} w(\mathrm{L},\Gamma)\,d\Gamma\,d\mathrm{L} - \iint\limits_{T(\mathrm{L}_n,\Gamma_{n-1})} w(\mathrm{L},\Gamma)\,d\Gamma\,d\mathrm{L}\Big) \qquad (19) \\ = \sum_{k=1}^{n-1} &\Big(W(\mathrm{L}_k,\Gamma_k) - W(\mathrm{L}_k,\Gamma_{k-1})\Big) \\ &+ \Big(W(\mathrm{L}_n,u_2) - W(\mathrm{L}_n,\Gamma_{n-1})\Big)\,. \qquad (20)\end{aligned}$$

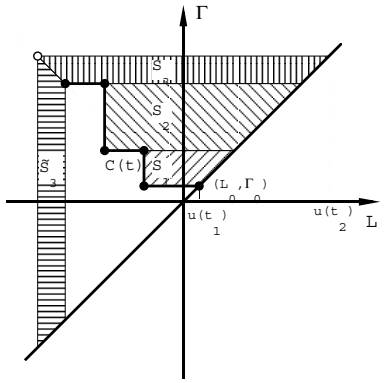

Fig. 5. When the input signal reaches outside of the memory function $\mathcal{C}(t)$, the integration must be between the lines L=-Γ and L=Γ, i.e. S_3 in the figure. The function $W(l,\gamma)$ can only be used in this case if it is assumed that the integrals over S_3 and $\tilde{S}_3$ are equal, i.e. symmetry applies.

The model is assumed to have a history described by the memory function $\mathcal{C}(t)$ to come to this result. If the input is increased beyond the last vertex of the memory function, yet not being saturated, it is here assumed that the material had not yet been 'magnetised', i.e. it has no memory. This means that the last term in (18) is an integral over a surface limited by the lines L=Γ and L=-Γ, i.e. S_3 in Fig. 5:

$$\iint\limits_{S_n} w(\mathrm{L},\Gamma)d\Gamma d\mathrm{L} = \int\limits_{\Gamma_n}^{u_2}\int\limits_{-\Gamma}^{\Gamma} w(\mathrm{L},\Gamma)d\mathrm{L}d\Gamma\,. \tag{21}$$

This term cannot be expressed with $W(l,\gamma)$ as is, but with the assumption of symmetry (7), the two integrals

$$\int\limits_{\Gamma_n}^{u_2}\int\limits_{-\Gamma}^{\Gamma} w(\mathrm{L},\Gamma)d\mathrm{L}d\Gamma \quad \text{and} \quad \int\limits_{u_2}^{\mathrm{L}_n}\int\limits_{\mathrm{L}}^{-\mathrm{L}} w(\mathrm{L},\Gamma)d\Gamma d\mathrm{L}\,, \tag{22}$$

i.e. the integrals over the two surfaces S_3 and $\tilde{S}_3$ in Fig. 5, are equal, which means that the sought integral is

$$\iint\limits_{S_n} w(\mathrm{L},\Gamma)d\Gamma d\mathrm{L} = \frac{1}{2}\Big(W(-u_2,u_2) - W(\mathrm{L}_n,\Gamma_{n-1})\Big)\,. \tag{23}$$

This completes the description how to calculate the difference of two outputs for an increasing input signal, and the total formula is given by

$$\begin{aligned}\Delta y_2 &= G(u_1,u_2,\mathcal{C}(t))\\ &= \sum_{k=1}^{n-1}\Big(W(\mathrm{L}_k,\Gamma_k) - W(\mathrm{L}_k,\Gamma_{k-1})\Big)\\ &\quad + \begin{cases}\Big(W(\mathrm{L}_n,u_2) - W(\mathrm{L}_n,\Gamma_{n-1})\Big)\,, & \mathrm{L}_n \neq -\Gamma_{n-1}\\ \frac{1}{2}\Big(W(u_2,u_2) - W(\mathrm{L}_n,\Gamma_{n-1})\Big)\,, & \mathrm{L}_n = -\Gamma_{n-1}\end{cases}\end{aligned} \tag{24}$$

So far the case when the input is increasing, $du/dt > 0$, has only been considered. With the same

reasoning as above, the difference of two outputs with decreasing input, $du/dt < 0$, is

$$\begin{aligned} y_2 - y_1 = &- \sum_{k=1}^{n-1} \Big(W(\mathrm{L}_k, \Gamma_k) - W(\mathrm{L}_{k-1}, \Gamma_k) \Big) \\ &- \begin{cases} \Big(W(u_2, \Gamma_n) - W(\mathrm{L}_{n-1}, \Gamma_n) \Big) , & \mathrm{L}_{n-1} \neq -\Gamma_n \\ \frac{1}{2} \Big(W(u_2, -u_2) - W(\mathrm{L}_{n-1}, \Gamma_n) \Big) , & \mathrm{L}_{n-1} = -\Gamma_n \end{cases} \end{aligned} \tag{25}$$

The similarities between (24) and (25) are obvious, which can be used to simplify an implementation. First, we need some new relations to be defined. The lower right part of the $\mathrm{L} - \Gamma$ plane ($\Gamma < \mathrm{L}$) is not used by the Preisach model so far. Therefore it is allowed to define $W(l, \gamma)$ in that region to be the negative function value mirrored in $\mathrm{L} = \Gamma$:

$$W(l, \gamma) = -W(\gamma, l) \, . \tag{26}$$

(This implies that $w(\mathrm{L}, \Gamma) = -w(\Gamma, \mathrm{L})$.) Further, an alternative memory function $\mathcal{C}'(t)$ is defined to be equal to $\mathcal{C}(t)$, except that the coordinates (L_k, Γ_k) change places. For the example in (17) this means

$$\mathcal{C}'(t) = \{ (\Gamma_2, \mathrm{L}_3), (\Gamma_2, \mathrm{L}_2), (\Gamma_1, \mathrm{L}_2), (\Gamma_1, \mathrm{L}_1), (\Gamma_0, \mathrm{L}_1), (\Gamma_0, \mathrm{L}_0) \} \, . \tag{27}$$

A general expression for the difference of two outputs then takes the following form:

$$\Delta y_2 = \begin{cases} G(u_1, u_2, \mathcal{C}(t)) \, , & du/dt > 0 \\ 0 \, , & du/dt = 0 \\ G(u_1, u_2, \mathcal{C}'(t)) \, , & du/dt < 0 \, . \end{cases} \tag{28}$$

The output from the numerical Preisach model is a number of sampled data $y_k = y(t_k)$ whose time instants coincide with the ones of the sampled input $u_k = u(t_k)$. The difference of the output from one time instant to another is calculated according to (24) and (28), so that the actual output is a cumulative sum of these differences

$$y_k = y_0 + \sum_{p=1}^{k} \Delta y_p \, . \tag{29}$$

The starting values y_0 and u_0 can be selected to any desired instant, such as demagnetised or saturated state. For the demagnetised state $y_0 = u_0 = 0$, but for the saturated state, y_0 must be calculated. It is then equal to the integral over S_{0+} and S_{0-} in Fig. 6 for positive and negative saturation, respectively.

$$y_0 = \begin{cases} \int_0^{\Gamma_s} \int_{-\Gamma}^{\Gamma} w(\mathrm{L}, \Gamma) d\mathrm{L} d\Gamma = \frac{1}{2} W(\mathrm{L}_s, \Gamma_s) \, , & \text{pos. sat.} \\ - \int_{\mathrm{L}_s}^{0} \int_{\mathrm{L}}^{-\mathrm{L}} w(\mathrm{L}, \Gamma) d\Gamma d\mathrm{L} = -\frac{1}{2} W(\mathrm{L}_s, \Gamma_s) \, , & \text{neg. sat.} \\ 0 \, , & \text{demagn.} \end{cases} \tag{30}$$

The expression above makes use of the assumptions that $\mathrm{L}_s = -\Gamma_s$ and that the symmetry (7) applies. A simple and straightforward estimate of $v(t)$ in this simulation context becomes

$$v_i = \Delta y_i \cdot f_s \tag{31}$$

if the sampling frequency f_s is large enough.

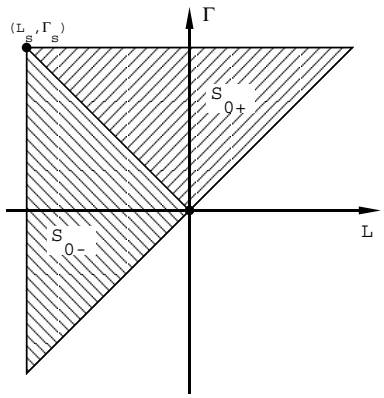

Fig. 6. The starting value y_0 can be chosen to any instant. The fully demagnetised state implies $y_0 = 0$, whereas positive and negative saturation corresponds integration over the surfaces S_{0+} and S_{0-}, respectively.

B. Energy Losses

The energy loss between two input values with a memory function $\mathcal{C}(t)$ such that the integration area is triangular can be implemented directly by taking half the value of (11) or by applying (13). In the case when an arbitrary memory function $\mathcal{C}(t)$ [and hence an arbitrary input signal] is to be applied, those methods cannot be used. A way to calculate the losses in the general case is to apply (10). By noting that the surface S corresponds to the sum of S_k's in Fig. 4, the calculation of the losses can be numerically implemented by applying

$$Q(u^-, u^+) = \frac{1}{2} \sum_{k=1}^{n(t)} \iint_{S_k(t)} w(\mathrm{L}, \Gamma)(\Gamma - \mathrm{L}) d\Gamma d\mathrm{L} \,. \tag{32}$$

This expression contains a number of double integrals which makes it computationally cumbersome.

An alternative is to proceed in a similar way as for the output signal $y(t)$ above. Such an analysis leads to that the losses between two input values u_1 and u_2 with an arbitrary $\mathcal{C}(t)$ as in (17) can be calculated by

$$\begin{aligned} Q(u_1, u_2) &= M(u_1, u_2, \mathcal{C}(t)) \\ &= \sum_{k=1}^{n-1} \Big(Q_W(\mathrm{L}_k, \Gamma_k) - Q_W(\mathrm{L}_k, \Gamma_{k-1}) \Big) \\ &+ \begin{cases} \Big(Q_W(\mathrm{L}_n, u_2) - Q_W(\mathrm{L}_n, \Gamma_{n-1}) \Big) \,, & \mathrm{L}_n \neq -\Gamma_{n-1} \\ \frac{1}{2} \Big(Q_W(u_2, u_2) - Q_W(\mathrm{L}_n, \Gamma_{n-1}) \Big) \,, & \mathrm{L}_n = -\Gamma_{n-1} \end{cases} \end{aligned} \tag{33}$$

when the input is increasing, $du/dt > 0$ and where $Q_W(\cdot)$ is defined in (13). Note that each term of the sum in (33), $(Q_W(\mathrm{L}_k, \Gamma_k) - Q_W(\mathrm{L}_k, \Gamma_{k-1}))$, involves only three integrations, since two of the integrals have the same integration variable.

Analogously to the analysis for the signal output $y(t)$ a general expression of the losses is found to be

$$Q(u_1, u_2) = \begin{cases} M(u_1, u_2, \mathcal{C}(t)) \,, & du/dt > 0 \\ 0 \,, & du/dt = 0 \\ M(u_1, u_2, \mathcal{C}'(t)) \,, & du/dt < 0 \end{cases} \tag{34}$$

Mathematically these proposed implementations may seem complicated, but the formulae (28) and (34) witness that a code can be very concise.

IV. Frequency Analysis

When the Preisach model is subject to a sinusoidal input signal, conclusions can be drawn about the frequency distribution of the output signal. A general expression of the Fourier transform of the output signal is derived here, and then a numerical simulation presented, from which we draw the conclusion that the Preisach model has a frequency contribution at all odd and only at odd harmonics of the fundamental input frequency.

Assuming a sinusoidal input signal (14) with an amplitude inferior to the saturation level,

$$U_0 < \min(|\mathrm{L}_s|, |\Gamma_s|)\,, \tag{35}$$

gives two different expressions for the output signal, depending on the the derivative of $u(t)$,

$$y(t) = \begin{cases} y(-U_0) + W(-U_0, u(t))\,, & du/dt \geq 0 \\ y(U_0) - W(u(t), U_0))\,, & du/dt < 0\,, \end{cases} \tag{36}$$

where $y(U_0)$ and $y(-U_0)$ are the outputs at maximum and minimum of the input $u(t)$, respectively. These extreme values are the negative of each other, since the input signal and the function $W(l, \gamma)$ both are symmetric. Furthermore, they are retrieved by using the equations derived for the numerical implementation in Section III [Use (30) with L_s=-U_0 and Γ_s=U_0.]

$$y(U_0) = -y(-U_0) = \frac{1}{2} W(-U_0, U_0) \tag{37}$$

Again using the symmetry (7), the output signal from the Preisach model in (36) can be merged into

$$y(t) = \mathrm{sgn}(-\frac{du}{dt}) \Big[y(U_0) - W(\mathrm{sgn}(-\frac{du}{dt})\, u(t), U_0) \Big]\,, \tag{38}$$

where the function $sgn(\cdot)$ is defined as

$$\mathrm{sgn}(x) = \begin{cases} 1\,, & x > 0 \\ 0\,, & x = 0 \\ -1\,, & x < 0\,. \end{cases} \tag{39}$$

It is now possible to apply the Fourier transform on the output:

$$Y(\omega) = \int_{-\infty}^{\infty} y(t) \mathrm{e}^{-j\omega t}\,. \tag{40}$$

As can be seen in (38), the output consists of a part that depends on the output at the input extrema exclusively, here denoted $y_A(t)$, and another part that depends on $W(l, \gamma)$, denoted $y_W(t)$. The same subscript is used for their corresponding Fourier transforms:

$$y(t) = y_A(t) - y_W(t), \tag{41}$$

$$Y(\omega) = Y_A(\omega) - Y_W(\omega) \tag{42}$$

By this separation, it is realised that $y_A(t)$ is in fact a square wave with amplitude $y(U_0)$. The Fourier transform for such a square wave is straight forward to calculate and takes the following form:

$$Y_A(\omega) = -j \frac{2y(U_0)}{\omega} \sum_{k=-\infty}^{\infty} \delta(\frac{\omega}{\omega_0} - 2p + 1) \tag{43}$$

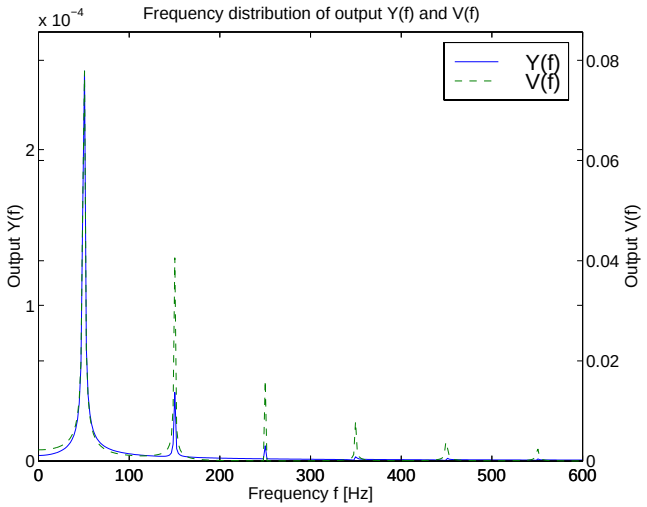

Fig. 7. Digital Fourier transform of simulated output from the Preisach model. The output $y(t)$ and $v(t)$ contain frequencies at all and only at odd harmonics of the fundamental input frequency, here 50 Hz.

where $\delta(\cdot)$ is the Dirac δ-function. The expression reveals that the square wave has sinusoidal contributions at all odd harmonics of the input frequency ω_0.

A general expression for the Fourier transform of the second part of the output signal, $y_W(t)$, cannot be retrieved without further information about $W(l,\gamma)$. However, it can be somewhat simplified by noting that the integral can be divided into a sum of partial integrals whose signs are determined by the negative derivative of the input signal, c.f. (38),

$$Y_W(\omega) = \sum_{k=-\infty}^{\infty} \Big[- \int_{(2k-1)\frac{\pi}{\omega_0}}^{2k\frac{\pi}{\omega_0}} W(-u(t),U_0)\mathrm{e}^{-j\omega t}dt + \int_{2k\frac{\pi}{\omega_0}}^{(2k+1)\frac{\pi}{\omega_0}} W(u(t),U_0)\mathrm{e}^{-j\omega t}dt \Big] \tag{44}$$

and that the negative input signal is equal to a time-delay of itself:

$$-u(t) = U_0\cos(\omega_0 t + \pi) = u(t + \frac{\pi}{\omega_0})\,. \tag{45}$$

The most general expression of $Y_W(\omega)$ without any assumptions on $W(l,\gamma)$ is then retrieved by combining (44) and (45) and applying a variable substitution:

$$Y_W(\omega) = (1 - \mathrm{e}^{j\pi\frac{\omega}{\omega_0}}) \sum_{k=-\infty}^{\infty} \int_{2k\frac{\pi}{\omega_0}}^{(2k+1)\frac{\pi}{\omega_0}} W(u(t),U_0)\mathrm{e}^{-j\omega t}dt\,. \tag{46}$$

With a known weighting function $W(l,\gamma)$, the integral in (46) is still difficult or even impossible to calculate analytically. A simulation with a sinusoidal input though gives us some useful information. Fig. 7 shows the digital Fourier transform of the output $y(t)$ and its derivative $v(t)$ of such a numerical simulation, which hence correspond to their frequency distribution,

$$Y(\omega) \quad \text{and} \quad V(\omega) = j\omega Y(\omega)\,. \tag{47}$$

From the simulation, we conclude that $Y(\omega)$ and $V(\omega)$ have contributions only at odd harmonics of the input,

$$Y(\omega) = \sum_{k=0}^{\infty} Y((2k+1)\omega_0)\,. \tag{48}$$

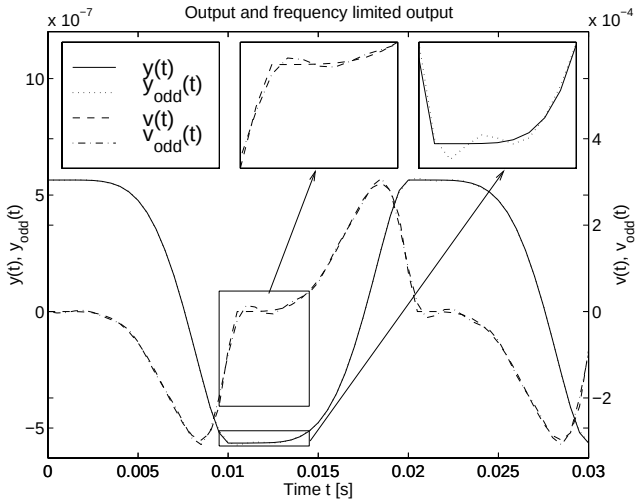

Fig. 8. Outputs $y(t)$ and $v(t)$ from a simulation of the Preisach model in time domain. The solid and dashed lines present correct outputs, whereas higher harmonics have been removed in the dotted and dash-dotted lines with a not fully reconstruction as result, as seen in the enlargements.

This means that in a noisy time-series measurement, we can extract these frequencies as long as their components are larger than the noise. A disadvantage with truncating the sum in (48) is that the signal cannot be fully reconstructed, but has some anomalies at the singularities, as seen in Fig. 8.

A. Identification of weighting function from time-series

The identification of weighting functions $w(\mathrm{L},\Gamma)$ or $W(l,\gamma)$ from first order transition curves suggested in [3] is tedious and in some cases not applicable, since some applications have not got a saturation mode. An alternative method is suggested here, where a number of sinusoids of different amplitude is used as input $u(t)$ and the weighting function is estimate from the output $y(t)$ or its differentiated version $v(t)$. Often data are full of noise so that their quality must be enhanced by some filtering technique. In view of the frequency analysis above (48), it is suggested here that only the odd harmonics are extracted from the output, for instance by a numerical lock-in method. This greatly enhances the signal to noise ratio. The resulting data $y_{odd}(t)$ can then be used to give raw estimates of the weighting functions $w(\mathrm{L},\Gamma)$ and $W(l,\gamma)$

$$\hat{\hat{W}}(-U_0, i(t)) = y(t) - y(t_{-U_0}) = \int_{t_{-U_0}}^{t} v(\tau)d\tau\,, \quad \frac{di(t)}{dt} > 0 \tag{49}$$

and

$$\hat{\hat{W}}(i(t), U_0) = y(t_{U_0}) - y(t) = -\int_{t_{U_0}}^{t} v(\tau)d\tau\,, \quad \frac{di(t)}{dt} < 0\,. \tag{50}$$

with an amplitude below the saturation as in (35). Fig. 9 depicts the result of such an estimation applied to high temperature superconductors [6], where several measurements of different input peak values U_0 were used to cover many values of the L–Γ plane.

The weighting function $w(\mathrm{L},\Gamma)$ can be computed directly with (5). However, differentiation of a signal containing noise gives an unreliable result, and it is, therefore, advantageous to use $W(l,\gamma)$ instead of $w(\mathrm{L},\Gamma)$ for time-series, since it gives less influence of the noise.

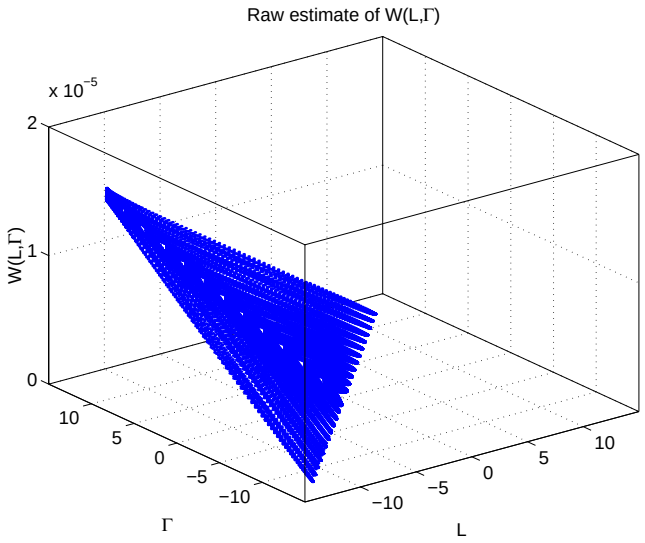

Fig. 9. Raw estimate of the weighting function $W(l,\gamma)$. The linear part of this estimates is dominant.

V. Conclusions

The classical Preisach model of hysteresis has been analysed. A simplified implementation using that there is no fundamental difference in increasing and decreasing inputs has been suggested. Solutions for both output signal, its differentiated version and instantaneous energetic losses have been derived. The initial 'magnetisation' can be taken to any value and there are no approximations for the fully 'demagnetised' state when symmetry applies.

A frequency analysis has shown that the output from a single frequency input contains all odd and only odd harmonics of the fundamental input frequency. A filtering technique by extracting only odd harmonics with amplitudes larger than the noise can, therefore, improve signal to noise ratio, even if the hysteresis cannot be fully reconstructed by a finite number of frequencies. A method that uses a number of sinusoids of different amplitude as input has been suggested for identification of the Preisach model weighting function.

References

[1] F. Preisach, *Z. Phys.*, pp. 277, 1935.
[2] M.A. Krasnoselskii and A.V. Pokrovskii, *Systems with Hysteresis*. Berlin, Germany: Springer Verlag, 1989.
[3] I.D. Mayergoyz, *Mathematical Models of Hysteresis*. New York, USA: Springer Verlag, 1991.
[4] L. D'Alessandro and A. Ferrero, "A Method for the Determination of the Parameters of the Hysteresis Model of Magnetic Materials", *IEEE Trans. on Instr. and Meas.*, vol. 43, no. 4, pp. 599–605, 1994.
[5] D. Djukic, "Modélisation des systèmes non-linéaires: ordre, adaptation des paramètres et hysterèse" *PhD thesis*, CIRC-EPFL, Lausanne, Switzerland, Nov. 1997.
[6] D. Djukic, M. Sjöström and B. Dutoit, "Preisach-type hysteresis modelling in Bi-2223 tapes", *Proc. 3rd European Conf. on Appl. Supercond.*, in press.
[7] M. Sjöström, D. Djukic and B. Dutoit, "Parametrised Preisach Modelling of Hysteresis in High Temperature Superconductors", *IEEE Trans. on Appl. Superconductivity*, submitted